Modeling for Chemical Vapor Deposition: Meso- and Microscale Models

Jürgen Geiser

Humboldt-Universität zu Berlin,
Department of Mathematics,
Unter den Linden 6, D-10099 Berlin, Germany
geiser@mathematik.hu-berlin.de

Abstract. In this paper we present modeling and simulation for chemical vapor deposition (CVD) on metallic bipolar plates.
In the models we discuss the application of different models to simulate the plasma-transport of chemical reactants in the gas chamber. We take into account one-dimensional models, that can be treated analytically under some assumptions and multi-dimensional models that are solved numerically with software packages.
Because of the multi-scaling problem of the physical behavior, we discuss adapted models in different domains and scales.
The near- and far-field contexts are based on large scales that can be treated with continuous models, such as convection-diffusion-reaction equations, and small scales that are based on chemical and molecular models, e.g. Boltzmann-equations.
The results are discussed with physical experiments to give valid models for the assumed growth of thin layers.

Keywords: Chemical vapor deposition, multi-scale problem, convection-diffusion equations.
AMS subject classifications. 35K25, 35K20, 74S10, 70G65.

1 Introduction

We carried out our study by simulating a low-temperature, low-pressure plasma that can be found in CVD processes. In recent years, due to research in producing high-temperature films by deposition, low-pressure processes have increased. The interest in standard applications to TiN and TiC are immense, but recently also deposition with new material classes known as MAX-phases became important. The MAX-phase consists of nano-layered terniar metal-carbides or -nitrides, where M is a transition metal, A is an A-group element (e.g. Al, Ga, In, Si, etc.) and X is C (carbon) or N (nitride).

We present a model for low-temperature and low-pressure plasma that can be used to implant or deposit thin layers of important materials. The so-called MAX-phases materials, see [1], are implanted in the metallic bipolar plates to

obtain a new material with non-corrosive and good metallic conductivity behavior.

We present different models of the implantation process. Firstly, the process in the plasma-reactor that transports the contaminants to the wafer-surface. We deal with a continuous flow model, while assuming a vacuum and a diffusion-dominated process. Secondly, the process at the wafer-surface is modeled by a heavy-particle problem with underlying drift. This model is more dealing with the atomic behavior; we do not allow $p = 0$. Thirdly, the topology of the thin-film structure is modeled by the coating-process.

To solve the model equations we use analytic, as well as numeric methods, for obtaining results to predict the growth of thin layers.

This paper is organized as follows:

In Section 2 we present our mathematical model and a possible reduced model for the further approximations. In Section 3 we discuss the time and spatial discretization methods. The numerical experiments are given in Section 4 and in Section 5 we summarize our results.

2 Mathematical Model

In the following the models are discussed in two directions of far-field and near-field problems:

1. Reaction-diffusion equations, see [11] (far-field problems);
2. Boltzmann-Lattice equations, see [23] (near-field problems).
3. Reaction equations, see [25] (kinetic problems).

The modeling for the far- and near-field problems are considered by the Knudsen number (Kn) which is the ratio of the mean free path λ over the typical domain size L. For small Knudsen numbers $Kn \approx 0.01-1.0$, we deal with a Navier-Stokes equation or with the convection-diffusion equation, see [17] and [21], whereas for large Knudsen numbers $Kn \geq 1.0$, we deal with a Boltzmann equation, see [22]. For the kinetic problems we only consider the chemical reaction between the species, see [25].

2.1 Model for Small Knudsen Numbers (Far-field Model)

When gas transport is physically more complex because of combined flows in three dimensions, the fundamental equations of fluid dynamics become the starting point of the analysis. For our models with small Knudsen numbers, we can assume a continuum flow, and the fluid equations can be treated with a Navier-Stokes or especially with a convection-diffusion equation.

Three basic equations describe the conservation of mass, momentum and energy that are sufficient to describe the gas transport in the reactors, see [22].

1. Continuity - the conservation of mass requires the net rate of the mass accumulation in a region be equal to the difference between the inflow and outflow rates.

2. Navier-Stokes - momentum conservation requires the net rate of momentum accumulation in a region to be equal to the difference between the in- and out-rate of the momentum, plus the sum of the forces acting on the system.
3. Energy - the rate of accumulation of internal and kinetic energy in a region is equal to the net rate of internal and kinetic energy by convection, plus the net rate of heat flow by conduction, minus the rate of work done by the fluid.

We will concentrate on the conservation of mass and assume that the energy and momentum are conserved, see [11]. Therefore the continuum flow can be described as a convection-diffusion equation given as:

$$\begin{aligned} \tfrac{\partial}{\partial t}c + \nabla F - R_g = 0, \text{ in } \Omega \times [0,T] \quad (1)\\ F = -D\nabla c, \\ c(x,t) = c_0(x), \text{ on } \Omega, \quad (2)\\ c(x,t) = c_1(x,t), \text{ on } \partial\Omega \times [0,T], \quad (3) \end{aligned}$$

where c is the molar concentration and F the flux of the species. D is the diffusivity matrix and R_g is the reaction term. The initial value is given as c_0 and we assume a Dirichlet boundary with the function $c_1(x,t)$ sufficiently smooth.

2.2 Model for Large Knudsen Numbers (Near-field Model)

The model assumes that the heavy particles can be described with a dynamical fluid model, where the elastic collisions define the dynamics and few inelastic collisions are, among other reasons, responsible for the chemical reactions.

To describe the individual mass densities as well as the global momentum and the global energy as dynamic conservation quantities of the system, corresponding conservation equations are derived from Boltzmann equations.

The individual character of each species is considered by mass-conservation equations and the so-called difference equations.

The Boltzmann equation for heavy particles (ions and neutral elements) is now given as:

$$\frac{\partial}{\partial t} n_s + \frac{\partial}{\partial \boldsymbol{r}} \cdot (n_s \boldsymbol{u} + n_s c_s) = Q_n^{(s)}, \quad (4)$$

$$\frac{\partial}{\partial t} \rho \boldsymbol{u} + \frac{\partial}{\partial \boldsymbol{r}} \cdot \left(\rho \boldsymbol{u}\boldsymbol{u} + nT\underline{\underline{I}} - \underline{\underline{\tau}}^*\right) = \sum_{s=1}^{N} q_s n_s \langle \boldsymbol{E} \rangle, \quad (5)$$

$$\begin{aligned} &\frac{\partial}{\partial t}\mathcal{E}_{\text{tot}}^* + \frac{\partial}{\partial \boldsymbol{r}} \cdot \left(\mathcal{E}_{\text{tot}}^* \boldsymbol{u} + \boldsymbol{q}^* + nT\boldsymbol{u} - \underline{\underline{\tau}}^* \cdot \boldsymbol{u}\right) \\ &= \sum_{s=1}^{N} q_s n_s \left(\boldsymbol{u} + \boldsymbol{c}_s\right) \cdot \langle \boldsymbol{E} \rangle - Q_{\mathcal{E},\text{inel}}^{(e)}, \end{aligned} \quad (6)$$

where ρ denotes the mass density, $\boldsymbol{u}$ is the velocity, and T the temperature of the ions. $\mathcal{E}^*_{\text{tot}}$ is the total energy of the heavy particles; n_s is the particle density of heavy particles species s; $\boldsymbol{q}^*$ is the heat flux of the heavy particle system; $\underline{\underline{\tau}}^*$ is the viscous stress of the heavy particle system; $\boldsymbol{E}$ is the electric field and $\overline{Q}_{\mathcal{E}}$ is the energy conservation.

Further, the production terms are $Q_n^{(s)} = \sum_r a_{\text{sign}} k_{\alpha,r} n_\alpha n_r$ with the rate coefficients $k_{\alpha,r}$.

We have drift diffusion for heavy particles in the following fluxes. The dissipative fluxes of the impulse and energy balance are linear combinations of generalized forces:

$$\boldsymbol{q}^* = \lambda_E \langle \boldsymbol{E} \rangle - \lambda \frac{\partial}{\partial \boldsymbol{r}} T - \sum_{s=1}^{N} \sum_{\alpha=1}^{N} \lambda_n^{(\alpha,s)} \frac{1}{n_s} \frac{\partial}{\partial \boldsymbol{r}} n_\alpha, \tag{7}$$

$$\underline{\underline{\tau}}^* = -\eta \left(\frac{\partial}{\partial \boldsymbol{r}} \boldsymbol{u} + \left(\frac{\partial}{\partial \boldsymbol{r}} \boldsymbol{u} \right)^\top - \frac{2}{3} \left(\frac{\partial}{\partial \boldsymbol{r}} \cdot \boldsymbol{u} \right) \underline{\underline{I}} \right), \tag{8}$$

$$\mathcal{E}^*_{\text{tot}} = \sum_{s=1}^{N} 1/2 \rho_s c_s^2 + 1/2 \rho u^2 + 3/2 n T. \tag{9}$$

where λ is the thermal diffusion transport coefficient. T is the temperature, n is the particle density.

Diffusions of the species are underlying to the given plasma and are described by the following equations:

$$\tfrac{\partial}{\partial t} n_s + \tfrac{\partial}{\partial \boldsymbol{r}} \cdot (n_s \boldsymbol{u} + n_s \boldsymbol{c}_s) = Q_n^{(s)}, \tag{10}$$

$$\boldsymbol{c}_s = \mu_s \langle \boldsymbol{E} \rangle - d_T^{(s)} \tfrac{\partial}{\partial \boldsymbol{r}} T - \textstyle\sum_{\alpha=1}^{N} D_n^{(\alpha,s)} \tfrac{1}{n_s} \tfrac{\partial}{\partial \boldsymbol{r}} n_\alpha. \tag{11}$$

The density of the species is in dynamical values and the species' transport and mass transport are subject to the following constraint conditions:

$$\textstyle\sum_s m_s n_s = \rho, \tag{12}$$

$$\textstyle\sum_s n_s m_s \boldsymbol{c}_s = 0. \tag{13}$$

where m_s is the mass of the heavy particle, n_s is the density of the heavy particle, and c_s is the difference velocity of the heavy particle.

Field Model

The plasma transport equations are Maxwell equations and are coupled with a field. They are given as:

$$\frac{1}{\mu_0} \nabla \times \boldsymbol{B}_{\text{dyn}} = -e n_e \boldsymbol{u}_e + \tilde{\boldsymbol{j}}_{\text{ext}}, \tag{14}$$

$$\nabla \cdot \boldsymbol{B}_{\text{dyn}} = 0, \tag{15}$$

$$\nabla \times \boldsymbol{E} = -\frac{\partial}{\partial t} \boldsymbol{B}_{\text{dyn}}, \tag{16}$$

where $\boldsymbol{B}$ is the magnetic field and $\boldsymbol{E}$ is the electric field.

2.3 Simplified Model for Large Knudsen Numbers (Near-field Model)

For the numerical analysis and for the computational results, we reduce the complex model and derive a system of coupled Boltzmann and diffusion equations.

We need the following assumptions:

$$\boldsymbol{q}^* = -\lambda \frac{\partial}{\partial \boldsymbol{r}} T, \tag{17}$$

$$\underline{\underline{\tau}}^* = 0, \tag{18}$$

$$\mathcal{E}^*_{\text{tot}} = 3/2nT, \tag{19}$$

$$Q^{(e)}_{\mathcal{E},\text{inel}} = \text{const}, \tag{20}$$

and obtain a system of equations:

$$\frac{\partial}{\partial t}\rho + \frac{\partial}{\partial \boldsymbol{r}} \cdot (\rho \boldsymbol{u}) = 0, \tag{21}$$

$$\frac{\partial}{\partial t}\rho \boldsymbol{u} + \frac{\partial}{\partial \boldsymbol{r}} \cdot \left(\rho \boldsymbol{u}\boldsymbol{u} + nT\underline{\underline{I}}\right) = \sum_{s=1}^{N} q_s n_s \langle \boldsymbol{E} \rangle, \tag{22}$$

$$\begin{aligned} &\frac{\partial}{\partial t} 3/2nT + \frac{\partial}{\partial \boldsymbol{r}} \cdot \left(3/2nT\boldsymbol{u} + \lambda \frac{\partial}{\partial \boldsymbol{r}} T + nT\boldsymbol{u}\right) \\ &= \sum_{s=1}^{N} q_s n_s \left(\boldsymbol{u} + \boldsymbol{c}_s\right) \cdot \langle \boldsymbol{E} \rangle - Q^{(e)}_{\mathcal{E},\text{inel}} \,. \end{aligned} \tag{23}$$

Remark 1. We obtain three coupled equations for the density, velocity and the temperature of the plasma. The equations are strong-coupled and decomposition can be done in the discretized form.

2.4 Chemical Reactions

For the modeling of the chemical reactions, it is important to understand the reactants. We discuss the kinetic problem by the following reactions, see [25]:

1.) Autocatalytic Reactions: $A \to P$

We obtain the term : $R_A = -kc_Ac_P$

$$\frac{\partial c_A}{\partial_t} = -kc_Ac_P, \tag{24}$$

where c_A and c_P are the concentrations of the chemical reactants A and P.

2.) Consecutive Reactions: $A \to B$, $B \to C$

We obtain the term : $R_A = -k_1c_A$, $R_B = k_1c_A - k_2c_B$, $R_C = k_2c_B$

$$\frac{\partial c_A}{\partial_t} = -k_1c_A, \tag{25}$$

$$\frac{\partial c_B}{\partial_t} = k_1c_A - k_2c_B, \tag{26}$$

$$\frac{\partial c_C}{\partial_t} = k_2c_B, \tag{27}$$

where c_A, c_B and c_C are the concentrations of the chemical reactants A, B and C.

A realistic reaction for the CVD-process is discussed in [3].

We have the following reaction equations:

$$\partial_t c_{tot} = -\lambda_1 \, c_{tot}, \tag{28}$$
$$\partial_t c_A = \lambda_1(1-\beta) \, c_{tot}, \tag{29}$$
$$\partial_t c_B = \lambda_1 \beta \, c_{tot} - \lambda_2 \, c_B, \tag{30}$$
$$\partial_t c_C = \lambda_2(1-\sigma) \, c_B - \lambda_3 \, c_C, \tag{31}$$
$$\partial_t c_D = \lambda_2 \sigma \, c_B, \tag{32}$$
$$\partial_t c_E = \lambda_3(1-\eta) \, c_C, \tag{33}$$
$$\partial_t c_F = \lambda_3 \eta \, c_C, \tag{34}$$

where c_{tot} are the total mass of the particles coming from the substrate, c_A, c_B, c_C, c_D and c_F are intermediate masses of the particles, c_A and c_F arrive at the targets.

Here, we have the following reaction-matrix :

$$\Lambda = \begin{pmatrix} -\lambda_1 & 0 & 0 & 0 & 0\,0\,0 \\ \lambda_1(1-\beta) & 0 & 0 & 0 & 0\,0\,0 \\ \lambda_1\beta & 0 & -\lambda_2 & 0 & 0\,0\,0 \\ 0 & 0 & \lambda_2(1-\sigma) & -\lambda_3 & 0\,0\,0 \\ 0 & 0 & \lambda_2\sigma & 0 & 0\,0\,0 \\ 0 & 0 & \lambda_2\sigma & 0 & 0\,0\,0 \\ 0 & 0 & 0 & \lambda_3(1-\eta) & 0\,0\,0 \\ 0 & 0 & 0 & \lambda_3\eta & 0\,0\,0 \end{pmatrix}, \tag{35}$$

The reaction equations can be solved by wave-form-relaxation method, see [24].

In the next section we discuss the discretization and solver methods.

3 Discretization and Solver Methods

For the numerical solutions we need to apply approximation methods, e.g. finite-difference methods and iterative-solver methods for the nonlinear differential equations.

3.1 Spatial Discretization Methods

For the spatial discretization methods we apply finite-difference methods, or finite-volume methods, see [18].

For the discretization of the transport equation we have to apply stable discretization schemes, e.g. upwind-methods, characteristics methods that follow the physical behavior of the model.

We discuss in the following the linear and nonlinear transport equations, with respect to the upwind schemes.

1.) The first equation is the linear transport equation:

$$\frac{\partial u}{\partial t} + v\nabla u = -\lambda u \ , \tag{36}$$

$$u(x,0) = u_0 \ , \tag{37}$$

where v is the velocity of the transport equation, u_0 is the initial condition of the equation, and we assume Dirichlet boundary conditions $u(x,t) = 0$ for $(x,t) \in \partial\Omega \times (0,T)$.

The analytical solution is given for the one-dimensional domain as:

$$u(x,t) = u_0(x - vt), \tag{38}$$

where $v \in \mathbb{R}^+$ and u_0 is the initial condition for $\lambda = 0$.

2.) The second equation is the nonlinear transport equation, e.g. the Burgers equation and given as:

$$\frac{\partial u}{\partial t} + u\nabla u = 0 \ , u(x,0) = sgn(x\sqrt{|2x|}) \ , \tag{39}$$

where u is unknown and so the velocity of the transport equation, $u(x,0)$ is the initial condition of the equation and we assume $(x,t) \in \partial\Omega \times (0,T)$.

The analytical solution is given for the one-dimensional domain as:

$$u(x,t) = sgn(x(\sqrt{t^2 + |2x|} - t)), \tag{40}$$

The solution is discontinuous, where the initial condition u_0 is continuous.

We assume to be far away from the boundaries, if not, we assume outflow conditions.

A stable discretization scheme of first order is given for the linear transport equation as:

$$u(x_i, t^{n+1} = u(x_i, t^n) - \frac{\Delta t \ v}{\Delta x} \begin{cases} u(x_i, t^n) - u(x_{i-1}, t^n), \ \text{for } \frac{\Delta t \ v}{\Delta x} \geq 0, \\ \\ u(x_{i+1}, t^n) - u(x_i, t^n), \ \text{for } \frac{\Delta t \ v}{\Delta x} \leq 0, \end{cases} \tag{41}$$

where for this explicit discretization method, we assume the CFL condition as $\frac{\Delta t v}{\Delta x} \leq 1$.

For the implicit discretization method, we replace the time of the transport-terms with t^{n+1} and obtain a linear equation system. This scheme is still stable for larger time steps, see [18].

A stable discretization scheme of first order is given for the nonlinear transport equation as:

$$u(x_i, t^{n+1} = u(x_i, t^n) - q \ \left(f(u(x_{i+1/2}, t^n)) - f(u(x_{i-1/2}, t^n))\right) \ , \qquad (42)$$

where for this explicit discretization method we have $q = \frac{\Delta t}{\Delta x}$ and for the Burger equation we have $f(u) = 1/2u^2$.

In this Godunovs method, see [12], the value $u(x_{i+1/2}, t^n)$ is given as :

$$u(x_{i+1/2}, t^n) = \begin{cases} u(x_i, t^n), \text{ for } f'(u(x_i, t^n)) > 0, f'(u(\xi_{i+1/2}, t^n)) > 0, \\ u(x_{i+1}, t^n), \text{ for } f'(u(x_{i+1}, t^n)) < 0, f'(u(\xi_{i+1/2}, t^n)) < 0, \\ u(x_{i+1/2}, t^n), \text{ solves } f'(u) = 0 \text{ for all other cases.} \end{cases} \qquad (43)$$

where $f'(u(\xi_{i+1/2}, t^n)) = \frac{f(u(x_{i+1}, t^n)) - f(u(x_i, t^n))}{u(x_{i+1}, t^n) - u(x_i, t^n)}$. For the value $u(x_{i-1/2}, t^n)$ we formulate in the same manner.

3.2 Time Discretization Methods

For the time-discretization methods, we apply finite-difference methods, Runge Kutta methods or other interpolation methods.

Runge-Kutta and IMEX methods For the time-discretization, we apply stable higher order methods, which can solve the stiff and coupled differential equations. We propose Runge-Kutta and IMEX (implicit-explicit) methods to solve such problems, see [2].

Runge-Kutta method

We use the implicit trapezoidal rule:

$$\begin{array}{c|cc} 0 & & \\ 1 & \frac{1}{2} & \frac{1}{2} \\ \hline & \frac{1}{2} & \frac{1}{2} \end{array} \quad . \qquad (44)$$

Furthermore we use the following Gauss-Runge-Kutta method:

$$\begin{array}{c|cc} \frac{1}{2} - \frac{\sqrt{3}}{6} & \frac{1}{4} & \frac{1}{4} - \frac{\sqrt{3}}{6} \\ \frac{1}{2} + \frac{\sqrt{3}}{6} & \frac{1}{4} + \frac{\sqrt{3}}{6} & \frac{1}{4} \\ \hline & \frac{1}{2} & \frac{1}{2} \end{array} \quad . \qquad (45)$$

Numerical experiments show that we can apply these methods for non-stiff problems, but not for stiff problems. Therefore we propose the IMEX methods.

Implicit-explicit methods The implicit-explicit (IMEX) schemes have been widely used for time integration of spatial discretized partial differential equations of diffusion-convection type. These methods are applied to decouple the implicit and explicit terms. Treating the convection-diffusion equation for example, one can use the explicit part for the convection and the implicit part for the diffusion term. In our application we can divide between the stiff and non-stiff term, so we apply the implicit part for the stiff operators and the explicit part for the non-stiff operators.

FSRK method

We propose the A-stable fractional-stepping Runge-Kutta (FSRK) scheme, see [2], of first and second order for our applications.
The tableau in the Butcher form is given as

$$\begin{array}{c|cccc|cccc} 1 & 1 & & & & 0 & & & \\ 1 & 1 & 0 & & & 0 & 1 & & \\ \frac{4}{9} & -\frac{88}{45} & 0 & \frac{12}{5} & 0 & 0 & \frac{5}{9} & 0 & \\ \frac{1}{3} & -\frac{407}{75} & 0 & -\frac{144}{25} & 0 & 0 & -\frac{31}{15} & 0 & \frac{12}{5} \\ \hline \text{order1} & 1 & 0 & 0 & 0 & 0 & 1 & 0 & 0 \\ \hline \text{order2} & \frac{1}{10} & 0 & \frac{9}{10} & 0 & 0 & \frac{1}{4} & 0 & \frac{3}{4} \end{array} \quad . \tag{46}$$

3.3 Iterative Solver Methods

For the coupled nonlinear differential equations, we apply linearization methods, see [16].

We deal with the following coupled differential equations:

$$\frac{\partial n_s}{\partial t} + u\frac{\partial n_s}{\partial x} = -\lambda_s n_s, \tag{47}$$

$$\rho\frac{\partial u}{\partial t} + \frac{\partial}{\partial x}\rho uu = q_s n_s \langle \boldsymbol{E} \rangle, \tag{48}$$

$$n_s(x,0) = n_s(x,0)\ ,\ x \in \Omega\ , \tag{49}$$

$$u(x,0) = u_0(x)\ ,\ x \in \Omega\ , \tag{50}$$

$$n_s(x,t) = 0\ ,\ x \in \partial\Omega \times (0,T)\ , \tag{51}$$

$$u(x,t) = 0\ ,\ x \in \partial\Omega \times (0,T)\ , \tag{52}$$

$$\tag{53}$$

where n_s is the density of the species s and u is the velocity of the density system, λ_s is the decay rate of the species s, ρ is the mass density and $\boldsymbol{E}$ is the electric field.

The initial conditions are given as $n_s(x,0)$ and $u(x,0)$ and are constant.

The coupled system can be solved iteratively by linearization:

Algorithm 1 *1.) Starting conditions are given as:*
$n_s(x_i,t^n), u(x_i,t^n)$ *with the spatial points* $i = 1,\ldots,p$,
$j = 1$ *and* $err \in \mathbb{R}^+$ *is a constant for the maximal error.*

2.) We compute the first equation
and assume the initial conditions $n_s(x_i, t^n)$ *are known.*

$$\frac{n_{s,j}(x_i, t^{n+1}) - n_s(x_i, t^n)}{\Delta t} + u_{j-1}(x_i, t^{n+1}) \frac{n_{s,j}(x_{i+1}, t^{n+1}) - n_{s,j}(x_i, t^{n+1})}{\Delta x} = -\lambda_s n_{s,j-1}(x_i, t^{n+1}), \tag{54}$$

we compute numerically the solution:
$n_{s,j}(x_i, t^{n+1})$ *for* $i = 1, \ldots, p$.

3.) We compute the second equation and insert the results of the first equation and assume the initial conditions $u(x_i, t^n)$ *are known:*

$$\rho \frac{u_j(x_i, t^{n+1}) - u(x_i, t^n)}{\Delta t} + u_j(x_i, t^n) \frac{u_j(x_{i+1}, t^{n+1}) - u_j(x_i, t^n)}{\Delta x} = q_s n_{s,j}(x_i, t^{n+1}) \langle \boldsymbol{E} \rangle, \tag{55}$$

we compute numerically the solution:
$u_j(x_i, t^{n+1})$ *for* $i = 1, \ldots, p$.

4.) We compute the maximal error of the two equations:

$$\max_{i=1}^{p}(|n_{s,j}(x_i, t^{n+1}) - n_{s,j-1}(x_i, t^n)|) = err_1, \tag{56}$$

$$\max_{i=1}^{p}(|u_j(x_i, t^{n+1}) - u_{j-1}(x_i, t^n)|) = err_2, \tag{57}$$

If $max(err_1, err_2) < err$ *then*
$n_{s,j}(x_i, t^{n+1})$ *and* $u_j(x_i, t^{n+1})$ *for* $i = 1, \ldots, p$ *is the solution.*
else $j = j + 1$ *and we go to step 2.)* .

In the next section we discuss the numerical experiments.

4 Experiment for the Plasma Reactor

In the following, we present different models based on the scales.

4.1 Mesoscopic Models

In the following, experiments we discuss the mesoscopic models. In such models we deal with a continuum flow problem.

Stagnant Layer Model In this model one assumes only the diffusion across a stagnant layer (mass-transfer-limited).

This model is used to simulate the gas transport of the concentration on a thin-film. The contamination is given in the vertical direction. Based on the time dependency, we can distinguish between a stationary and instationary model.

We model the transport of the contaminants by a convection-diffusion equation that is given as:

$$\begin{aligned} \frac{\partial c}{\partial t} = D(\frac{\partial^2 c}{\partial x^2} + \frac{\partial^2 c}{\partial y^2}) - v\frac{\partial c}{\partial x} \quad &\text{in } (x,y,t) \in [0,1] \times [0,b] \times [0,\infty], \\ c(x,y,0) = 1 \quad &\text{on } (x,y) \in 0 \times [0,b], \\ c(x,y,t) = 0 \quad &\text{on } (x,y,t) \in [0,1] \times 0 \times [0,\infty], \\ \frac{\partial c}{\partial y} = 0 \quad &\text{on } (x,y,t) \in [0,1] \times b \times [0,\infty]. \end{aligned} \tag{58}$$

where c is the concentration of the contaminant, D is the diffusion parameter of the idealized gas, v is the velocity in x the direction of the gas. The dimension of the chamber is given as $\Omega = [0,1] \times [0,b]$.

The following assumption is necessary:
we assume a large flow rate or a large chamber, $vb >> D$.

The parameters are given for a first stationary experiment $t \to \infty$:

$$\begin{aligned} b &= 1.0, \\ v &= 0.1, \\ D &= 0.01. \end{aligned}$$

For the stationary solution we obtain the following analytical solution:

$$c(x,y) = \frac{4}{\pi}\sin(\frac{\pi y}{2b})\exp(-\frac{\pi^2 D x}{4vb^2}), \tag{59}$$

where $(x,y) \in [0,1] \times [0,1]$.

For the instationary solution we obtain the following analytical solution:

$$c(x,y,t) = \frac{4}{\pi}\sin(\frac{\pi y}{2b})\exp(-\frac{\pi^2 D(x-vt)^2}{4vb^2}), \tag{60}$$

where $(x,y,t) \in [0,1] \times [0,b] \times [0,T]$, with $T \in \mathbb{R}^+$.

The growth rate is given as:

$$g = \frac{m_{\text{film}}}{m_{\text{gas}}}\frac{1}{\rho_{\text{film}}}j(x), \tag{61}$$

where $j(x)$ is the mass flux at substrate:

$$j(x) = \frac{2}{b}D\exp(-\frac{\pi^2 D x}{4vb^2})$$

We simulate the analytical solution for the concentration and the growth.

Figure 1 presents the model in two dimensions.

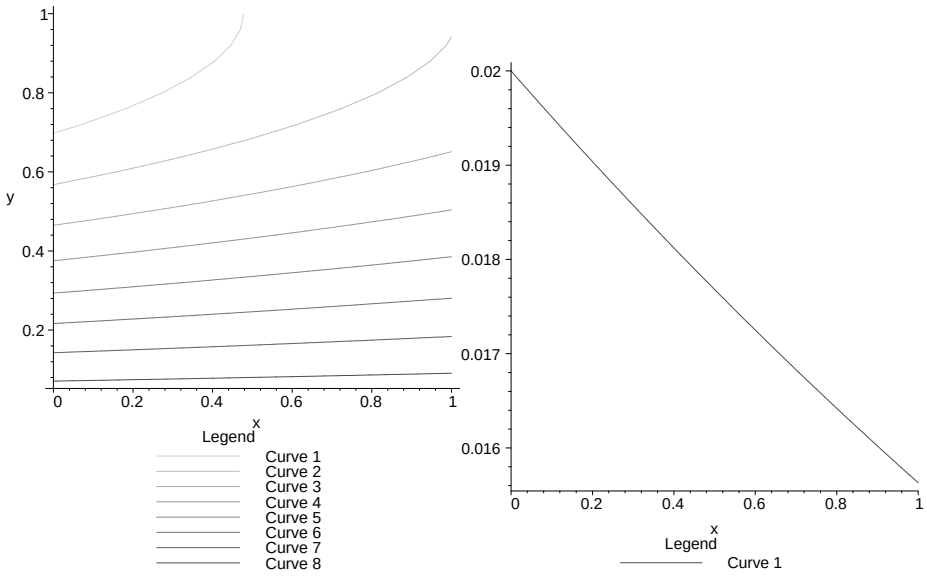

Fig. 1. Two-dimensional experiment of the stagnant layer. Left: gas concentration in the domain; right: growth rate of the thin film (parameters: $b = 1, v = 0.1, D = 0.01$, other parameters 1).

Remark 2. The model can be used to have an overview of horizontal gas flowing across the thin layer. We can compute the growth rate depending on the amount of the velocity and diffusion. The simulations are done with Maple and Mathematica.

Pulse Injection (Vertical Layer Model) This model is used to simulate the transport with the x-axis. The pulse injection simulates a finite source and we can also rotate the model about 90-degrees to obtain the reactor configuration.

We have the following assumptions:
In this model we assume that we have a pulse injection into a vertical gas chamber.

The convection-diffusion-reaction equation is given as:

$$\frac{\partial c}{\partial t} = (D_L \frac{\partial^2 c}{\partial x^2} + D_T \frac{\partial^2 c}{\partial y^2}) - v\frac{\partial c}{\partial y} - \lambda c, \text{ in } (x, y, t) \in [0, 1] \times [0, b] \times [0, \infty] \quad (62)$$

$$c(x, y, 0) = c_0 \text{ on } (x, y) = (x_0, y_0),$$

$$c(x, y, 0) = 0 \text{ on } (x, y) \in \Omega \backslash \{(x_0, y_0)\},$$

$$c(x, y, t) = 0 \text{ on } (x, y, t) \in \partial\Omega \times [0, \infty],$$

where c is the concentration of the contaminant, the diffusion parameters are given as $D_L = \alpha_L v$, $D_T = \alpha_T v$, v is the velocity in x direction. The decay rate is given as λ. The domain is given as: $\Omega = [0,1] \times [0,1]$.

The parameters are given for the instationary experiment $t \to \infty$:

$$\begin{aligned} T &= 10.0, \\ v &= 0.1, \\ D &= 0.01, \\ c_0 &= 1.0. \end{aligned}$$

The analytical solution is given as:

$$c(x,y,t) = \frac{c_0}{4\pi\sqrt{\alpha_L \alpha_T}(vt\pi)} \tag{63}$$

$$\exp(-\frac{((x-x_0)-vt)^2}{4\alpha_L vt}) \exp(-\frac{(y-y_0)^2}{4\alpha_T vt}) \exp(-\lambda t), \tag{64}$$

where $(x,y) \in [0,1] \times [0,1]$, $t \in [0,T]$.

The growth rate is:

$$g = \frac{m_{\text{film}}}{m_{\text{gas}}} \frac{1}{\rho_{\text{film}}} j(x), \tag{65}$$

where $j(x)$ is the mass flux at substrate:

$$j(y) = -D_L \frac{\partial c(x,y,t)}{\partial x})|_{x=0.1}.$$

We simulate the analytical solution for the concentration and the growth.

Figure 2 presents the model in two dimensions.

Remark 3. The model can be used to have an overview of vertical gas flowing with a pulse injection across the thin layer. We can compute the growth rate depending on the amount of the velocity and diffusion. The simulations are done with Maple and Mathematica.

Point-like Continuous Inflow (Vertical Layer Model) This model is used to simulate the transport with the x-axis and to have an infinite source. We can also rotate the model about 90-degrees to obtain the reactor configuration.

We have the following assumptions:
In this model, we assume that we have a point-like continuous inflow into a vertical gas chamber.

The convection-diffusion equation is given as:

$$\frac{\partial c}{\partial t} = (D_L \frac{\partial^2 c}{\partial x^2} + D_T \frac{\partial^2 c}{\partial y^2}) - v\frac{\partial c}{\partial x} + q(t), \text{ in } (x,y,t) \in [0,1] \times [0,b] \times [0,\infty], \tag{66}$$

$$c(x,y,0) = 0 \text{ on } (x,y) \in 0 \times [0,b],$$

$$c(x,y,t) = 0 \text{ on } (x,y,t) \in [0,1] \times 0 \times [0,\infty],$$

$$\frac{\partial c}{\partial y} = 0 \text{ on } (x,y,t) \in [0,1] \times b \times [0,\infty],$$

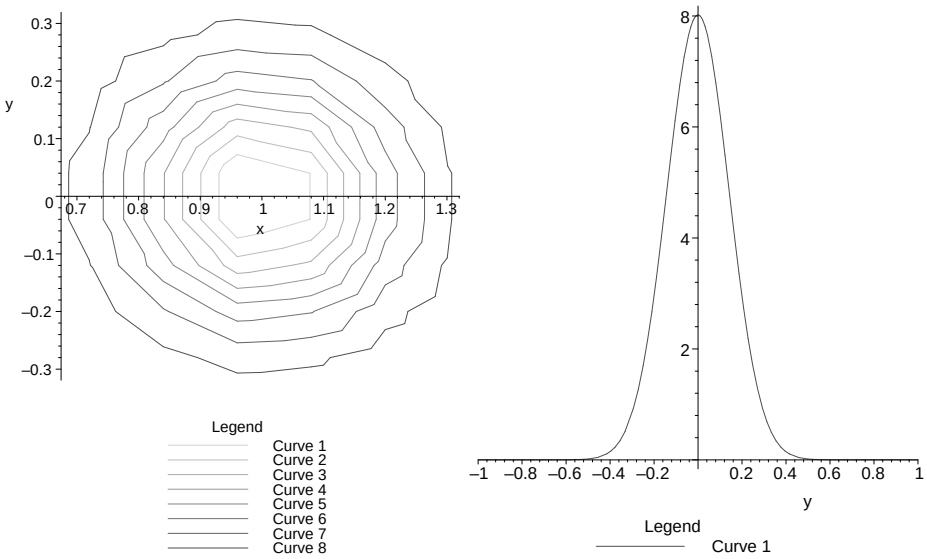

Fig. 2. Two-dimensional experiment of the vertical gas flow for the thin layer. Left: gas concentration in the domain; right: growth rate of the thin film (parameters : $v = 0.1, D = 0.01, \lambda = 0$, other parameters 1).

where $q(t) = \begin{cases} q_s/T, t \leq T \\ 0, \quad t > T \end{cases}$ is the permanent inflow source at point $(x, y) = (0, 0)$ and q_s is the source-rate and T is the time for the injection. Further, c is the concentration of the contaminant, the diffusion parameters are given as $D_L = \alpha_L v$, $D_T = \alpha_T v$, v is the velocity in x direction. The decay rate is given as λ. The domain is given as $\Omega = [0, 1] \times [0, 1]$.

The parameters are given for a first experiment:

$$\begin{aligned} T &= 10.0, \\ v &= 0.1, \\ D &= 0.01, \\ q_s &= 1.0. \end{aligned}$$

The analytical solution is given as:

$$c(x, y, t) = \frac{q_s}{4\pi\sqrt{\alpha_l \alpha_T}} \exp(\frac{x}{2\alpha_L}) W(\frac{r^2}{4\alpha_L v t}, \frac{r\gamma}{2\alpha_L}), \tag{67}$$

where $(x, y) \in [0, 1] \times [0, 1]$, $t \in [0, T]$, and with the Hantush function we have:

$$W(a_1, a_2) = \int_{a_1}^{\infty} \frac{1}{\zeta} \exp(-\zeta - \frac{a_2^2}{4\zeta}), \tag{68}$$

where:

$$\gamma = \sqrt{1 + 4\alpha_L \lambda / v},$$
$$r = \sqrt{x^2 + (\alpha_L/\alpha_T) y^2}.$$

The growth rate is given as:

$$g = \frac{m_{\text{film}}}{m_{\text{gas}}} \frac{1}{\rho_{\text{film}}} j(x), \tag{69}$$

where $j(x)$ is the mass flux at substrate:

$$j(x) = -D \frac{\partial c(x, y, t)}{\partial x})|_{x=0.1}.$$

where $t = 100.0$. We simulate the analytical solution for the concentration and growth.

Figure 3 presents the model in two dimensions.

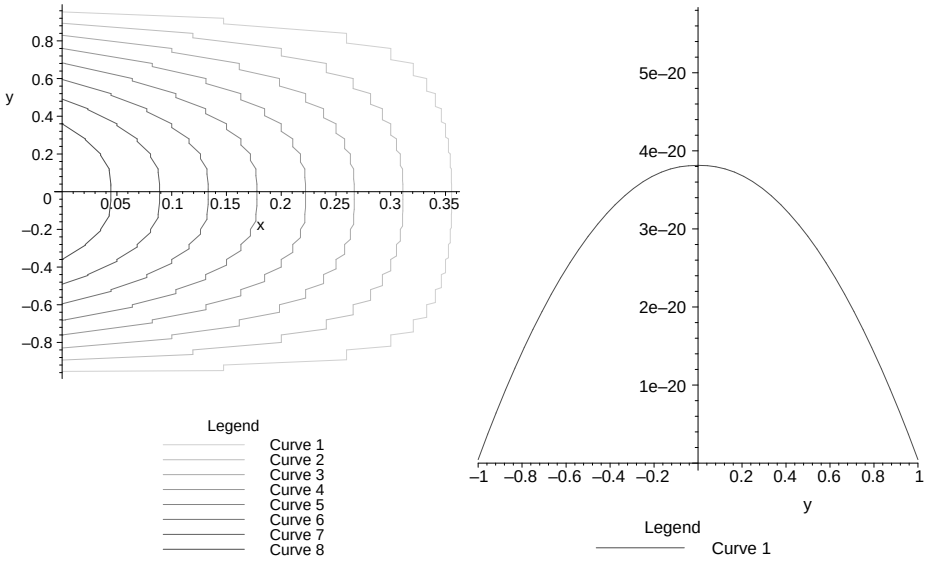

Fig. 3. Two-dimensional experiment of the vertical gas flow into the thin layer. Left: gas concentration in the domain; right: growth rate of the thin film (parameters : $v = 0.1, D = 0.01$, other parameters 1).

Remark 4. The model can be used to have an overview of vertical gas flowing across the thin layer. We can compute the growth rate depending on the amount of the velocity and diffusion. The simulations are done with Maple and Mathematica.

4.2 Microscopic Models

In this section we deal with the microscopic models that deal with discrete behaviour of single particles.

One-dimensional Particle Model In this model we can discuss the particle transport of ions or electrons.

Based on the one-dimensional problem we can derive an analytical solution.

$$-\frac{\partial^2 h_\xi}{\partial \xi^2} = (\kappa^2 - \gamma^2) h_\xi \ , \tag{70}$$

$$h_\xi(0) = h_0 \ , \tag{71}$$

where $h = n/n_0$ is the ion or electron density, κ^2 is the ionisation rate, γ is the constant of separation, and ξ is a radial, dimensionless coordinate.

The analytical solution can be derived as:

$$h_\xi = \cos(\tilde{\kappa}\xi) + \tilde{\kappa}^{-1} \sin(\tilde{\kappa}\xi) \ , \tag{72}$$

where $\tilde{\kappa} = \sqrt{\kappa^2 - \gamma^2}$.

The parameters are given for a first experiment:

$$\kappa \in [0, 0.2],$$
$$\gamma \in [0.01, 1.0].$$

Figure 4 presents the profile of the plasma density in one dimension.

Plasma Potential The plasma potential describes the potential at the sheath edge.

The equations given as:

$$U_{pl} = U_{pl}^0 - \frac{kT_e}{e} ln(-1 - \xi/2 + \sqrt{(\xi/2)^2 + 4\xi}) \ ,$$

where U_{pl}^0 is the plasma potential at the sheath edge. The normalized distance is given as $\xi = (h - d_s)/\Gamma$.

Heavy-Particle Model (Drift and Difference Velocity) For the heavy particle model, we have a drift and difference velocity for the particles in the system.

Mass-conservation of the Heavy Particles:

In a first experiment we assume a constant drift velocity and constant energy, and obtain the following equations:

$$\partial_t n_s + \nabla \cdot \mathbf{v} \ n_s = \sum Q_n^{(s)} \text{ in } \Omega \times (0, T) \ , \tag{73}$$

$$n_{s,0}(x) = u_s(x, 0) \ \text{ on } \Omega \ , \tag{74}$$

$$s = 1, \ldots, m \ , \tag{75}$$

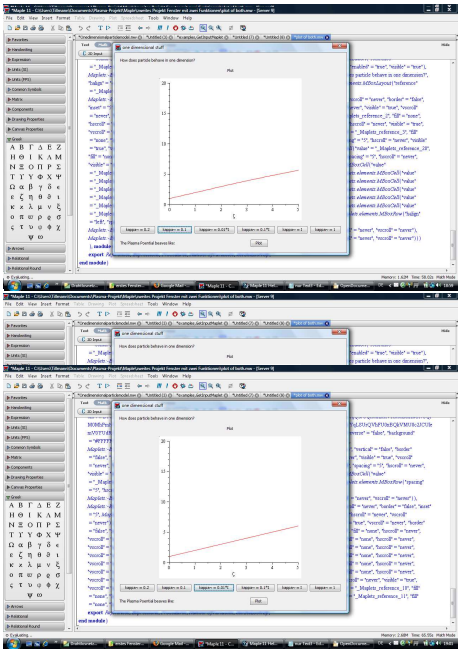

Fig. 4. 1D experiment of the heavy particle transport: $\kappa = 0, 0.1, 0.2, \gamma = 0.01, 0.1, 1$.

where m is the number of species in the system. The unknowns are the particle densities $n_s = n_s(x,t)$ which are considered in $\Omega \times (0,T) \subset \mathbb{R}^n \times \mathbb{R}^+$, where n is the spatial dimension. The exchange term is given as $Q_n^{(s)}$ and the velocity is given as v and is constant.

We consider the one-dimensional problem:

$$\partial_t n_s + v\, \partial_x n_s = \lambda n_s \text{ in } \Omega \times (0,T)\,, \tag{76}$$

$$n_{s,0}(x) = \begin{cases} 1 \text{ for } 0.1 \leq x \leq 0.2 \\ 0 \qquad\quad else \end{cases}\,, \tag{77}$$

where $\Omega = [0,1]$ and the time-interval $(0,T) = (0,10)$. The constant velocity is given as $v = 0.05$ and the decay-rate is given as $\lambda = 0.001$ and is constant.

The analytical solution is given as:

$$u(x,t) = \begin{cases} u_0(x - vt)\exp(-\lambda t) \text{ for } x \in [vt + 0.1, vt + 0.2] \\ 0 \qquad\qquad\qquad\qquad\qquad\quad \text{else} \end{cases}\,, \tag{78}$$

where u_0 is the initial condition.

We have the following simulations, with $\Delta t = 0.01$ and we fulfill the CFL condition:

$\Delta t\, v/\Delta x \leq 1$.

Further, the maximum error at the end-time $t = T$ is given as:
$\text{err} = |u_{num} - u_{ana}| = \max_{i=1}^{p} |u_{num}(x_i, t) - u_{any}(x_i, t)|$

Δx	$\text{err} = u_{num} - u_{ana}$
0.1	7.3724e-001
0.01	2.7910e-002
0.001	2.1306e-003

Table 1. Numerical results for the heavy particle mass transport.

Figure 6 presents the profile of the mass-conservation in the one-dimensional experiment.

Mass- and impulse-conservation of the heavy particles:

In a second experiment we assume a constant energy and obtain the following equations:

$$\partial_t n_s + \nabla \cdot \mathbf{v}\, n_s = \sum Q_n^{(s)} \text{ in } \Omega \times (0,T)\,, \tag{79}$$

$$n_{s,0}(x) = u_s(x,0) \text{ on } \Omega\,, \tag{80}$$

$$\partial_t \rho \mathbf{v} + \nabla \cdot \rho \mathbf{v}\mathbf{v} = \sum q_s n_s < E > \text{ in } \Omega \times (0,T)\,, \tag{81}$$

$$\mathbf{v}_0(x) = \mathbf{v}(x,0) \text{ on } \Omega\,, \tag{82}$$

$$s = 1, \ldots, m\,, \tag{83}$$

where m is the number of species in the system. The unknowns are the particle densities $n_s = n_s(x,t)$ which are considered in $\Omega \times (0,T) \subset \mathbb{R}^n \times \mathbb{R}^+$, where n is the spatial dimension. The exchange term is given as $Q_n^{(s)}$ and the unknown's drift velocity is given as $\mathbf{v}$. We have also a constant electric field $< E >$.

We consider the one-dimensional coupled equation system:

$$\partial_t n_s + \partial_x (n_s u) = -\lambda n_s \text{ in } \Omega \times (0,T)\,, \tag{84}$$

$$n_{s,0}(x) = \begin{cases} 1 \text{ for } 0.1 \le x \le 0.2 \\ 0 \qquad else \end{cases}\,, \tag{85}$$

$$\partial_t \rho u + \partial_x \rho u^2 = \lambda n_s < E > \text{ in } \Omega \times (0,T)\,, \tag{86}$$

$$u_0(x) = \begin{cases} 1 \text{ for } x \ge 0 \\ 0 \text{ for } x \le 1 \end{cases}\,, \tag{87}$$

where the unknowns are the particle densities $n_s = n_s(x,t)$ which are considered in $[0,1] \times (0,10) \subset \mathbb{R}^n \times \mathbb{R}^+$. The exchange term is given as $\lambda = 0.001$ and the constant electrical field is given as $< E >= 1$.

We have the following simulations, with $\Delta t = 0.01$ and apply the Godunovs method.

Figure 6 presents the profile of the mass- and impulse equations in one dimension.

5 Conclusions and Discussions

We present continuous and discrete models, due to the far-field or near-field effect. Based on the different scale models, we could predict the flow of the reacting chemicals on the scale of the chemical reactor. For the mesoscopic scale model, we discussed the discretization and solver methods. Numerical examples are presented to discuss the influence of near-continuum regime at the thin film. Far-field experiments have presented the transport of the mass and impulse of the kinetic problem. In future, we will analyze the validity of the models with physical experiments.

References

1. M.W. Barsoum and T. El-Raghy. *Synthesis and Characterization of a Remarkable Ceramic: Ti_3SiC_2.* J.Am.Ceram.Soc., 79, 1953–1956, 1996.
2. J.C. Butcher. *Numerical Methods for Ordinary Differential Equations. John Wiley & Sons Ltd, Chichester*, 2003.
3. D.J. Christie. *Target material pathways model for high power pulsed magnetron sputtering.* J. Vac. Sci. Technol., A 23 (2), 330–335, 2005.
4. I. Farago and Agnes Havasi. *On the convergence and local splitting error of different splitting schemes.* Eötvös Lorand University, Budapest, 2004.
5. K.-J. Engel, R. Nagel, *One-Parameter Semigroups for Linear Evolution Equations.* Springer, New York, 2000.
6. I. Farago. *Splitting methods for abstract Cauchy problems.* Lect. Notes Comp.Sci. 3401, Springer Verlag, Berlin, 2005, pp. 35-45
7. I. Farago, J. Geiser. *Iterative Operator-Splitting Methods for Linear Problems.* Preprint No. 1043 of the Weierstrass Institute for Applied Analysis and Stochastics, Berlin, Germany, June 2005.
8. J. Geiser. *Numerical Simulation of a Model for Transport and Reaction of Radionuclides.* Proceedings of the Large Scale Scientific Computations of Engineering and Environmental Problems, Sozopol, Bulgaria, 2001.
9. J. Geiser. *Gekoppelte Diskretisierungsverfahren für Systeme von Konvektions-Dispersions-Diffusions-Reaktionsgleichungen.* Doktor-Arbeit, Universität Heidelberg, 2003.
10. J. Geiser. *Discretisation methods with analytical solutions for convection-diffusion-dispersion-reaction-equations and applications.* Journal of Engineering Mathematics, published online, October 2006.
11. M.K. Gobbert and C.A. Ringhofer. *An asymptotic analysis for a model of chemical vapor deposition on a microstructured surface.* SIAM Journal on Applied Mathematics, 58, 737–752, 1998.
12. S.K. Godunov and V.S. Ryabenkij. *Theory of Difference Schemes: An Introduction.* North-Holland, Amsterdam, Interscience (Wiley), New York, 1964.
13. Ch. Grossmann and H.-G. Ross. *Numerik partieller Differentialgleichungen.* Teubner Studienbücher, Mathematik, 1994.
14. S. Karaa. *High-Order Compact ADI Methods for Parabolic Equations.* Journal of Computers and Mathematics with Applications, Vol. 52, Iss. 8-9, 1343–1356, 2006.
15. S. Karaa. *High-Order Difference Schemes for 2-d Elliptic and Parabolic Problems with Mixed Derivatives.* Wiley InterSciences, published online, October 2006.

16. C.T. Kelly. *Iterative Methods for Linear and Nonlinear Equations.* Frontiers in Applied Mathematics, SIAM, Philadelphia, USA, 1995.
17. H.H. Lee. *Fundamentals of Microelectronics Processing* McGraw-Hill, New York, 1990.
18. R.J. LeVeque. *Finite Volume Methods for Hyperbolic Problems.* Cambridge Texts in Applied Mathematics, Cambridge, UK, 2002.
19. M.A. Lieberman and A.J. Lichtenberg. *Principle of Plasma Discharges and Materials Processing.* Wiley-Interscience, AA John Wiley & Sons, Inc Publication, Second edition, 2005.
20. Chr. Lubich. *A variational splitting integrator for quantum molecular dynamics.* Report, 2003.
21. S. Middleman and A.K. Hochberg. *Process Engineering Analysis in Semiconductor Device Fabrication* McGraw-Hill, New York, 1993.
22. M. Ohring. *Materials Science of Thin Films.* Academic Press, San Diego, New York, Boston, London, Second edition, 2002.
23. T.K. Senega and R.P. Brinkmann. *A multi-component transport model for non-equilibrium low-temperature low-pressure plasmas.* J. Phys. D: Appl.Phys., 39, 1606–1618, 2006.
24. S. Vandewalle. *Parallel Multigrid Waveform Relaxation for Parabolic Problems.* B.G. Teubner, Stuttgart, 1993.
25. K.R. Westerterp, W.P.M. van Swaaij and A.A.C.M. Beenackers. *Chemical Reactor Design and Operation.* John Wiley & Sons, Chichester, New York, 1984.

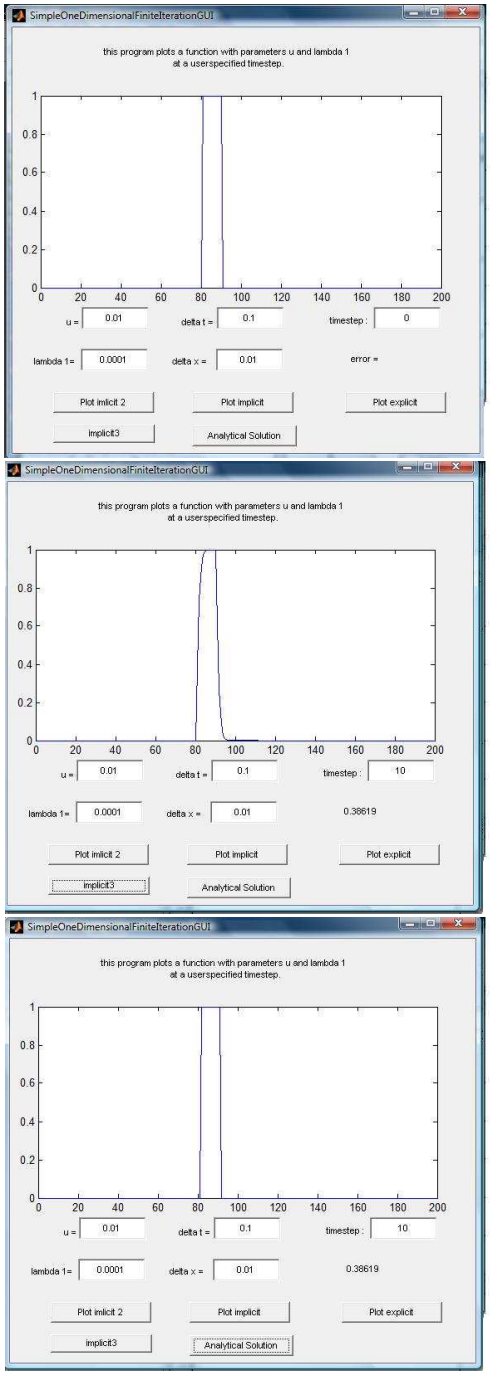

Fig. 5. One-dimensional experiment for heavy particle transport; mass-conservation; initial condition and signal at further time steps.

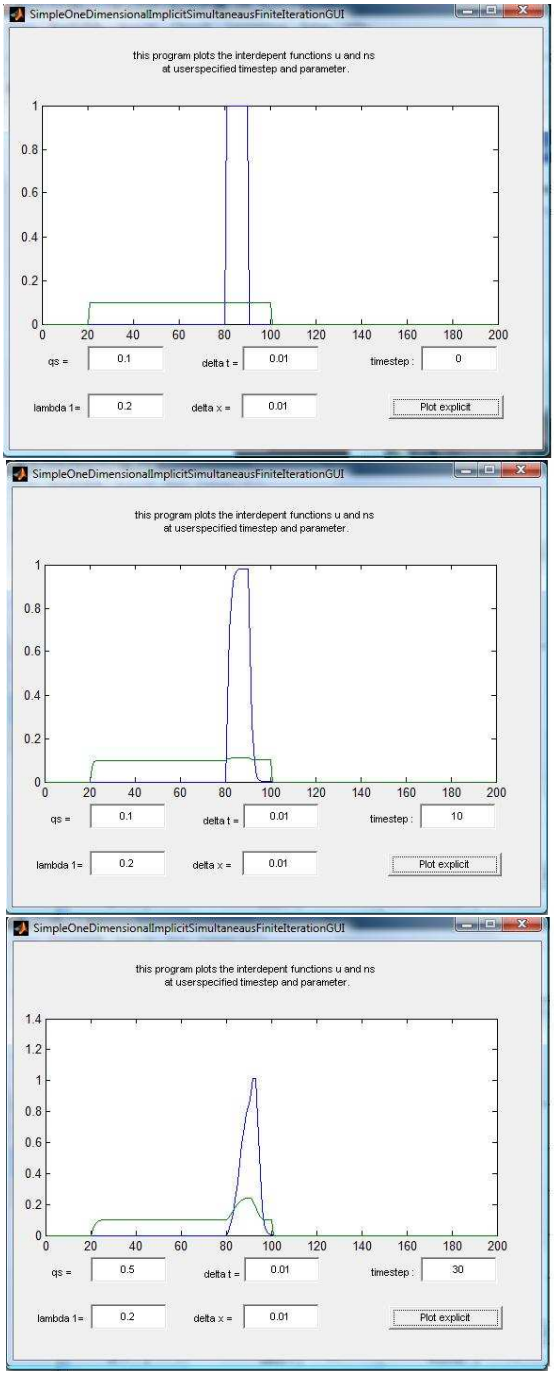

Fig. 6. One-dimensional experiment for heavy particle transport; mass- and impulse-conservation; initial condition and signal at further time steps.